Journal of Pharmaceutical Sciences 113 (2024) 463–470

Contents lists available at ScienceDirect

Journal of Pharmaceutical Sciences

journal homepage: www.jpharmsci.org

Pharmaceutical Nanotechnology

Anti-Melanoma Activity of Single Intratumoral Injection of ZnPc Micelles Mixed With *in situ* Gel in B16 Bearing Mouse

Jing-hua Xu[a,*], Chun-xue Zhang[a], Ai-jun Cang[b], Ran Yan[c], Shi-wen Liu[d], Rui Liu[c], Nv-jie Zou[d], Shao-ning Wang[d], Hui Xu[c,*], Lin-sen Li[e,*]

[a] School of Life Science and Biopharmaceutics, Shenyang Pharmaceutical University, No. 26 Huatuo Road, Benxi 117004, China
[b] Department of Pharmacy, The People's Hospital of Liaoning Province, Shenyang 110016, China
[c] School of Pharmacy, Shenyang Pharmaceutical University, No. 26 Huatuo Road, Benxi 117004, China
[d] School of Pharmaceutical Engineering, Shenyang Pharmaceutical University, No. 26 Huatuo Road, Benxi 117004, China
[e] School of International Education, Shenyang Medical College, No. 146 Huanghe North Street, Shenyang 110034, China

ARTICLE INFO

Article history:
Received 5 July 2023
Revised 12 October 2023
Accepted 12 October 2023
Available online 16 October 2023

Keywords:
Photodynamic therapy
ZnPc
Intratumoral injection
Thermosensitive gel
Anti-melanoma

ABSTRACT

Photodynamic therapy (PDT) is a potential treatment strategy for melanoma. As a second-generation photosensitizer, Zinc phthalocyanine (ZnPc) has many advantages for anti-tumor PDTs, such as strong absorption in the red and near infrared regions, high photo and chemical stability, etc. However, ZnPc has a poor water solubility and is apt to aggregate due to the π-π interaction between molecules, which limits its applications. In this study, various solvents and surfactants were screened for dissolving ZnPc and preparing ZnPc@SDC-TPGS micelle and thermosensitive *in situ* gel. After the cytotoxic effects of thermosensitive gels on PDT were tested, the antitumor effects on PDT of them in mice by intratumoral injection were evaluated, including body weight, and tumor weight, volume and morphology. The cell death pathway and the relationship of reactive oxygen species yield with apoptotic rate of tumor cells induced by ZnPc *in situ* gel were investigated. The results were that N-methyl-pyrrolidone (NMP) mixed with 2 % SDC and aqueous solution containing 2 % TPGS and 2 % SDC were used to synthesize ZnPc@SDC-TPGS micelle and the thermosensitive *in situ* gel. The cytotoxic effects of thermosensitive gels showed good tumor suppression of ZnPc@SDC-TPGS *in situ* gel and no toxicity of the blank gel. Intratumoral injection *in situ* gel containing 3 μg ZnPc under irradiation demonstrated good tumor inhibition in mice with melanoma. Apoptosis has been established as the primary pathway of cell death, and the production of reactive oxygen species (ROS) plays a crucial role in cellular apoptosis induced by ZnPc@SDC-TPGS *in situ* gel. In conclusion, the intratumoral injection of ZnPc@SDC-TPGS thermosensitive *in situ* gel provides a promising local treatment option for melanoma.

Introduction

Malignant melanoma is one of skin cancers with the highest mortality due to its high aggressiveness and unpredictable evolution.[1] At early stage of melanoma, surgical excision, radiation therapy and chemotherapy are the standard and effective treatments. For advanced melanoma, the resistance to existing therapies leads to poor prognosis.[2] Consequently, patients are often given high dose of radiation or chemotherapy, which is associated with high toxicity. Therefore, localized therapies, *e.g.* local radiotherapy or chemotherapy, intratumoral injection of oncolytic virus,[3] photothermal therapy or photodynamic therapy, etc. are induced as primary or adjuvant treatments for melanoma.

Photodynamic therapy (PDT), an effective treatment strategy for tumor,[4] is a therapeutic procedure utilizing reactive oxygen species (ROS). Singlet oxygen ($^1O_2$) is generated by irradiating nontoxic photosensitizers (PSs) with near-infrared light at suitable wavelength, resulting in cell death though apoptosis, necrosis or autophagy.[5] Ideal PSs not only have high absorption coefficients in the near-infrared region for deep tissues penetration, but also possess high photostability for minimize photo-bleaching.[6] Phthalocyanines (Pcs) and their derivatives are promising second-generation PSs due to their long triplet lifetimes, high fluorescence and triplet quantum yield. Zn (II) phthalocyanine (ZnPc) has demonstrated promising anti-tumor effect as a PDT.[4] However, the clinical application of intravenous ZnPc injection was hindered due to the intermolecular π-π interaction of ZnPc, leading to high polar and low solubility.[7] N,N-dimethylformamide (DMF), N-methyl-pyrrolidone (NMP), dimethyl sulfoxide (DMSO) and their aqueous solutions are often used to improve the solubility of

* Corresponding authors.
E-mail addresses: lilinsen@symc.edu.cn, xuhui_lab@163.com (L.-s. Li).

https://doi.org/10.1016/j.xphs.2023.10.020

PSs.[8] In this study, NMP was used as organic phase to increase the solubility of ZnPc. NMP has been approved by the US Food and Drug Administration (FDA) for treatment of prostate cancer and is a good solvent and penetration enhancer for delivery of hydrophobic photosensitizers into tumor tissue in PDT.[9]

To improve solubility and prevent aggregation of ZnPc, chemical modification or nanocarriers, such as, nanoparticles, liposomes, vesicles, and micelles, etc., have been investigated for effectively delivery to tumor issue.[10,11] D-α-tocopheryl polyethylene glycol 1000 succinate (TPGS), a nonionic-amphiphilic polymer, is extensively used in nanoparticulate formulation as emulsifier, stabilizer, penetration enhancer, solubilizer and protective agent.[12] TPGS improves the permeability of drugs due to the P-glycoprotein inhibition in the multi-drug resistant cancer cells. Many TPGS nanoparticles with a high drug encapsulation have demonstrated benefits in improving cellular uptake and therapeutic efficacy. However, the high critical micelle concentration (CMC) value and insufficient drug loading capacity of TPGS micelles limited its application for drug delivery.[13] Therefore, mixed micelles were prepared by adding other amphiphilic substances, such as pluronic and sodium deoxycholate, to enhance the loading capacity, stability, and oral bioavailability.[5,14] Sodium deoxycholate (SDC), a bile salt, is a commonly used biosurfactant to form micellar systems.[5,15] SDC combined with other surfactants[16] or polymers[17] can form various micellar structures with enhanced drug loading efficiency and micellar stability.

Systemic administration of anti-cancer drugs leads to low drug exposure in tumor location and side effects, including poor therapeutic efficacy and patients' complaints in clinic. Therefore, active or passive tumor targeting systems for accurately delivering antitumor substances to the cancerous lesion are essential.[18] Local tumor administration strategies, for example, intratumoral or intracavitary chemotherapy, have been gained clinical acceptance for the treatment of solid tumors such as gliomas and melanoma.[19,20] Intratumoral injection of chemotherapeutic agents enhances cytotoxicity and antitumor efficacy by increasing the concentration and retention of chemotherapeutic agents in the tumor and reduces the distribution of the drugs to normal tissues and organs.[21] However, due to the pressure difference produced by interstitial fluid pressure in solid tumors, the intratumorally injected agents could be squeezed out through the pinprick and causing drug leakage.[22] Therefore, thermosensitive polymers, which transform from sol to gel state at body temperature, are used to increase retention time of drugs in tumor and local drug concentration.[23] For example, Pluronic F127 (F127) hydrogel is a widely studied temperature responsive drug-delivery system for local tumor administration therapy.[24]

In this study, an intratumoral injection of ZnPc micelle-based thermo-sensitive *in situ* gel was designed and evaluated regarding physical characteristics, and *in vitro* and *in vivo* PDT behaviors. The mixed micelles composed of SDC and TPGS improve tissue penetration, and water-solubility and stability of ZnPc within tumors, while the thermo-sensitive gel for increasing drug retention in tumor. The intratumoral injection of thermo-responsive gel combined PDT was expected to perform better anti-tumor efficiency and provide a novel choice for cancer therapy in the future.

Schematic diagram: Preparation of ZnPc@Micelle and ZnPc@Gel, and their *in vivo* anti-tumor PDT via intratumoral injection.

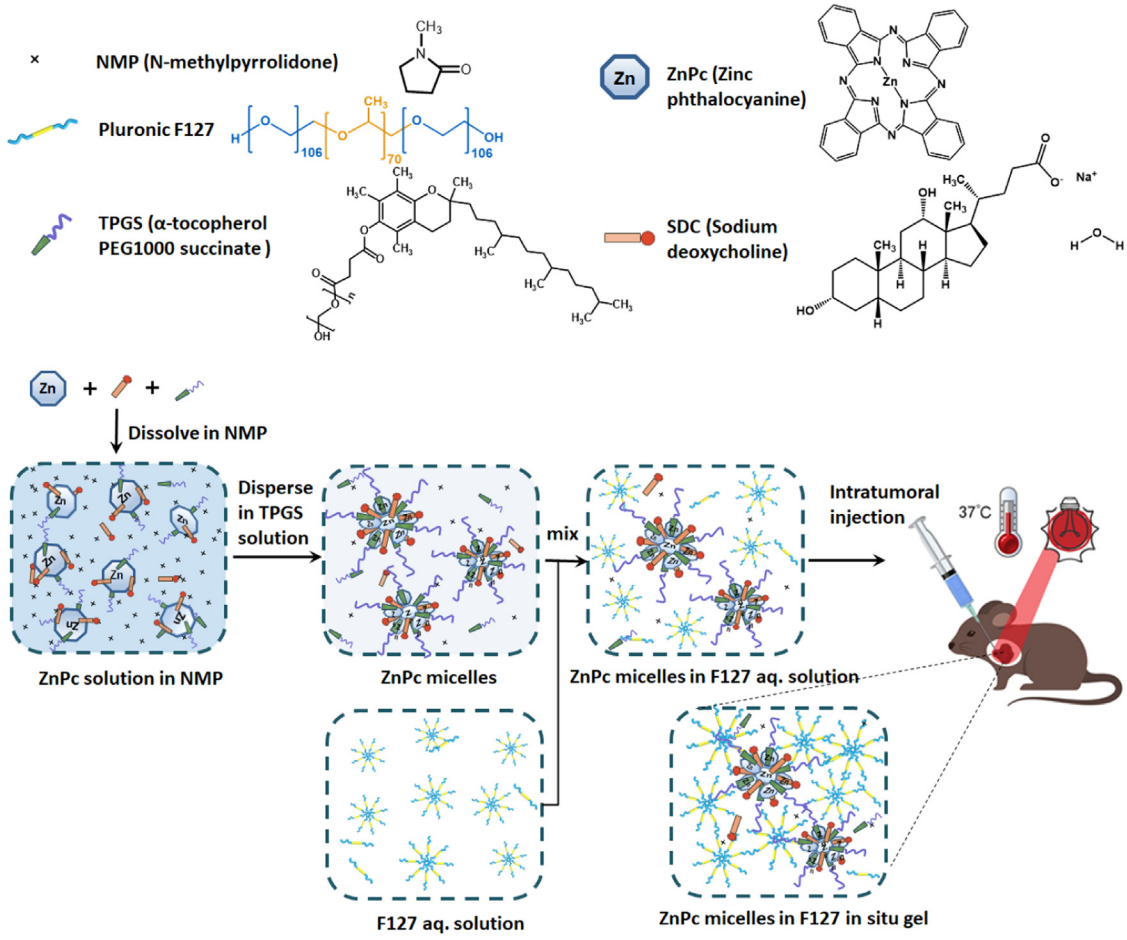

Experiments

Materials and Animals

ZnPc, SDC, NMP, PVP K30 and F127 were kindly donated by BASF (Berlin, Germany); Tween 80 was purchased from Sinopharm Chemical Reagent Co.,Ltd. (Shanghai, China); TPGS was received from PMC Isochem (France); Polyethylene glycol 200 (PEG200); MTT cell proliferation and cytotoxicity assay kits were purchased from Beyotime Biotechnology Co.,Ltd. (Shanghai, China); All other chemicals and solvents were of analytical or chromatographic grade.

B16 mice-derived cancer cell line (melanoma) was purchased from the Cell Bank of Chinese Academy of Science (Shanghai, China); Male C57BL/6 mice (18–20 g, 6 weeks) were obtained from the Experimental Animal Center of Shenyang Pharmaceutical University (Shenyang, China). All the animal experiments were performed in accordance with institutional guidelines.

Solubility of ZnPc

ZnPc 8 mg was added into 1 ml of solvent including NMP, PEG 200, purified water, NMP mixed with 2 % (w/v) SDC, NMP mixed with 2 % (w/v) Tween-80, NMP mixed with 2 % (w/v) PVP K30, NMP mixed with 2 % (w/v) TPGS. After ultrasonic treatment for 30 min, the mixtures were incubated at 25 °C for 48 h in a water-bath shaker. Samples were centrifuged at 5000 r/min for 10 min, 0.5 mL supernatant was diluted into 4.5 mL NMP mixed with 2 % SDC. The concentration of ZnPc (extinction coefficient, ε=1.7 $\times$ 10^5 M^{-1} cm^{-1}) was assayed using a UV–vis spectrophotometer (Wanyi Technology Co.,Ltd, China) at 670 nm.

Preparation of ZnPc@SDC-TPGS Micelles (ZnPc@Micelle) and Thermosensitive in situ *Gel Containing ZnPc Micelles (ZnPc@Gel)*

ZnPc 8 mg and TPGS 100 mg were dissolved in 1 ml NMP mixed with 2 % SDC (w/v) via ultrasonic treatment. 0.5 ml of ZnPc solution was mixed in 4.5 mL aqueous solution containing 2 % TPGS (w/v) and 2 % SDC (w/v) under vigorous stirring to obtain ZnPc@Micelle. To prepare ZnPc@Gel, 0.5 ml of ZnPc solution was mixed with 4.5 mL aqueous solution containing 2 % TPGS (w/v), 2 % SDC (w/v) and 25 % F127 (w/v). Cooled samples were filtrated through microporous membrane (Milipore®, USA) with a pore size of 0.22 μm and stored at 4°C in a refrigerator with light proofing.

Characterization of the ZnPc@Micelle and ZnPc@Gel

UV–vis spectrum of ZnPc dispersion in aqueous surfactant solution were measured. 0.1 mL of ZnPc 8 mg/mL NMP mixed with 2 % of various polymer surfactants (PVP K30, SDC, TPGS and Tween-80) was dropped into 10 mL of aqueous solution, containing a 2 % of surfactant, under vigorous stirring. After ultrasonic treatment for 30 min, the mixture was centrifuged at 5000 r/min for 10 min. The supernatant was analyzed using UV–vis spectrophotometer in purified water in a wavelength rage between 400 nm to 800 nm. The particle size, size distribution and zeta-potential of ZnPc@Micelle and ZnPc@Gel solution after dilution in purified water were measured with the Laser Particle Size Analyzer (Particle Sizing Systems Co., Ltd, USA). The UV–vis spectrum and fluorescence spectrum (excitation wavelength 670 nm) of ZnPc@Micelle and ZnPc@Gel were measured using the UV–vis spectrophotometer and the fluorescence detector (SpectraMax M3, Molecular Devices Co., Ltd, China), respectively.

In vitro *Release*

In vitro drug release behavior of ZnPc@Gel was tested by a "direct release" method. Briefly, 0.5 ml of gel was placed into a 2 ml test tube, after equilibrium at 37 °C for 10 min (sol-gel conversion) 1 ml of release medium (2 % (w/v) SDC aqueous solution) was added. The tube was then capped and incubated in a reciprocating water bath shaking incubator (Zhicheng Inc., China) vibrated at 50 rpm and 37 ° C. 1 ml of sample was withdrawn at predetermined time intervals and replaced with fresh medium. The concentration of ZnPc was analyzed at 670 nm using a UV–vis spectrophotometer. The experiments were performed in triplicate.

In vitro *Cytotoxicity Assay*

The cytotoxicity of the *in situ* gels with or without loading of ZnPc was determined in B16 cell line using MTT assay method. Cells at a density of 1 $\times$ 10^5 cells per ml at a volume of 100 μL per well were seeded in 96-well plates and incubated overnight at 37 °C under 5 % CO_2. Control experiments were carried out using the complete growth culture medium only (serving as nontoxic control). The cells were incubated with blank gel or ZnPc@Gel at various ZnPc concentrations (1.25, 2.5, 5.0, 10.0, 20.0, 40.0 μM) for a period of 4 h, respectively. Different concentrations of blank gel were the results of parallel dilution according to the ZnPc@Gel using serum. The control group was filled with culture medium only. The cells were then washed twice with sterile PBS before addition of fresh medium. The plates were illuminated with a light of 1.5 J/cm^2 (at a density of 100 mW/cm^2 for 5 min) using a 670 nm LED laser device (Uniglory Electronics Co., Ltd. China) before placing in the incubator; dark toxicity was measured in parallel. After culturing for 16 h, the medium from each well was removed and the cells were washed twice with PBS. 180 μL of the complete growth culture medium and 20 μL MTT solution (5 mg/ml in PBS pH 7.4) were then added to each well. After 4 h of incubation at 37°C and 5 % CO_2, the media were removed. The formazan was dissolved in 100 μL DMSO and then incubated for 10 min at 37°C. The amount of formazan was then determined from the optical density at 490 nm by a Thermo Scientific Microplate Reader (Multiskan GO, Finland). The cell phototoxicity or dark toxicity curves were plotted as a function of the ZnPc concentrations.

In vivo *PDT Pharmacodynamics*

ZnPc@Gel *in vivo* PDT were studied in B16 tumor xenograft model via single-point intratumoral injection. C57BL/6 mice (4~6 weeks) weight 20~22 g were used in this study. Briefly, 8 $\times$ 10^5 B16 cells were subcutaneously injected into the right flank of the mice. When the tumor volumes of mice were about 200 mm^3, the mice were randomly assigned into 7 groups (n = 5). All the groups received the following intratumoral injection. Control Group: SDC-TPGS blank gel (equilibrated to 30 μL gel/mouse); G1UI group: low dose group of ZnPc@Gel with illumination (equilibrated to 1 μg ZnPc/mouse); G3UI group: middle dose group of ZnPc@Gel with illumination (equilibrated to 3 μg ZnPc/mouse); G10UI group: high dose group of ZnPc@Gel with illumination (equilibrated to 10 μg ZnPc/mouse); M3UI group: group of ZnPc@Micelle with illumination (equilibrated to 3 μg ZnPc/mouse); G3 group: middle dose group of ZnPc@Gel without illumination (equilibrated to 3 μg ZnPc/mouse); Doxorubicin (DOX) Group: DOX thermosensitive *in situ* gel without illumination (equilibrated to 200 μg DOX/mouse). 2 h after intratumoral injection, the mice of illumination group were irradiated with a 670 nm laser (power density of 42.5 mW/cm^2, Qingdao Sundynamic Biomedical Technology Co., Ltd. China) at the tumor site for 5 min. To avoid any tissue damage by heating, the laser treatment was carried out with 2 h interval for another 5 min. The illumination was performed every

two days. Tumor diameters were measured using a caliper, and tumor volumes were determined by the following equation: tumor volume = length × width^2/2. Tumor sizes and body weights of mice were measured every two days. 15 days after injection, mice were scarified and the tumor was dissected and weighed to calculate the tumor inhibition rate.

The tumors were collected, sectioned and stained with hematoxylin and eosin (H&E) staining. Histological images were captured by optical microscope to observe the tumor necrotic regions.

Statistical Analysis

All data were expressed as Mean±SD. Statistical significance was determined by one-way ANOVA followed by Tukey's Post hoc tests. $P<0.05$ was considered statistically significant.

Results

Preparation and Characterization of ZnPc@Micelle and ZnPc@Gel

In this study, ZnPc-loaded micelles, formed by mixing the ZnPc solution in NMP with aqueous nonionic surfactant solution, were dispersed into a thermosensitive gel. ZnPc is insoluble in water and many organic solvents. High solubility solvent is the important precondition for self-assembling with surfactant for ZnPc-loaded micelles with a high drug loading. The solubility of ZnPc in different solvents was measured and the results were listed in Table 1. Compared with PEG 200 and purified water, NMP had a better solubility of ZnPc of 2.638 ± 0.316 mg/mL. To improve the solubility and prevent aggregation of ZnPc in NMP, several surfactants, including 2 % SDC (w/v), 2 % PVP K30 (w/v), 2 % Tween 80 (w/v) and 2 % TPGS (w/v), were mixed with NMP. All surfactants evaluated improved the solubility of ZnPc in NMP. NMP mixed with 2 % SDC (w/v) showed the best solubility for ZnPc of 9.887 ± 0.485 mg/mL among all tested solvents and was over 3 folds of that without SDC.

High dispersion of ZnPc in aqueous medium is important for PDT because the aggregation of ZnPc reduces the capacity of energy transference. Surfactants dissolved in aqueous solution improve the dispersibility of ZnPc. SDC, PVP K30, Tween 80 and TPGS were investigated regarding their effects on the dispersibility of ZnPc. As shown in Fig. 1, the aqueous solution containing 2 % TPGS showed characteristic absorption peak at 670 nm, which corresponded to the high dispersion of ZnPc. This result indicated that the addition of TPGS in aqueous solution did not change the absorption characteristics of ZnPc and improved the dispersibility of ZnPc. Therefore, SDC and TPGS were used as surfactants to improve the solubility and the stability of ZnPc, and were used as the materials for self-assembling ZnPc micelles.

The ZnPc@Micelle and ZnPc@Gel samples stored at 4°C had no precipitate over 7 days. To investigate the dispersion of the ZnPc in aqueous solution, the UV–vis spectrum and fluorescence emission spectrum of ZnPc@Micelle and ZnPc@Gel were measured. As shown in Fig. 2a and b, the characteristic absorption peak and strong fluorescent signal of ZnPc indicated a high dispersibility of ZnPc in aqueous

Table 1
Solubility of ZnPc in different solvents.

Solvents	Solubility, mg/mL
NMP	2.638±0.316
PEG200	0.038±0.008
Purified water	insoluble
2 % SDC in NMP	9.887±0.485
2 % PVP K30 in NMP	3.050±0.294
2 % Tween-80 in NMP	3.698±0.361
2 % TPGS in NMP	3.298±0.664

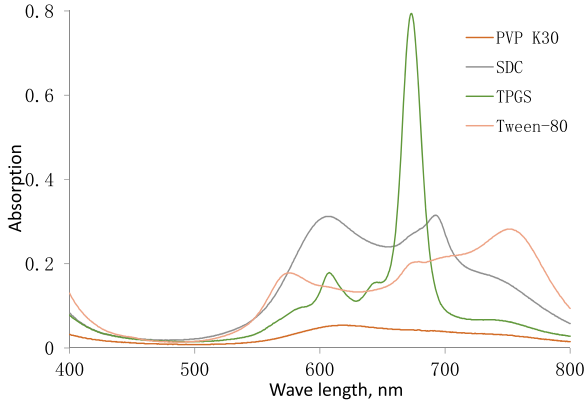

Fig. 1. UV–vis spectrum of ZnPc dispersion in various surfactant aqueous solutions.

solution. As shown in Fig. 2c, ZnPc@Gel had a low viscosity at 15°C and transformed to gel state at 37°C. This result indicated that at body temperature, ZnPc was more likely retained inside the tumor tissue after ZnPc@Gel intratumor injection. The release behaviors of ZnPc@Gel were investigated in aqueous solution containing 2 % SDC at 37 °C. The accumulated release of ZnPc increased with a time-dependent pattern and was more than 63 % at 4.5 h (Fig. 2d).

Particle size distributions and zeta-potential values of ZnPc@Micelle and ZnPc@Gel solution were detected. The average size distribution and zeta-potential value for ZnPc@Micelle were 107.60 nm and −22.6 mV, respectively, and were 47.03 nm and −5.34 mV for ZnPc@Gel, respectively.

In vitro *Cytotoxicity*

To investigate photodynamic antitumor effects of ZnPc@Gel *in vitro*, the phototoxicity and toxicity in dark condition of *in situ* gel with or without ZnPc (blank gel) on B16 cell line were studied. As shown in Fig. 3, the cell viability of B16 significantly decreased in response to ZnPc@Gel treatment with illumination (Fig. 3a), with no decrease in dark condition (Fig. 3b). Higher concentrations (5 μM, 10 μM, and 20 μM) of ZnPc in *in situ* gel were associated with increased photodynamic effects. All concentrations of the blank *in situ* gel showed no toxicity to B16 cells with or without illumination (Fig. 3c and d). The results demonstrated that ZnPc in *in situ* gel had good cytotoxicity after irradiation and no toxicity in dark condition.

Pharmacodynamics

The anti-tumor efficacy of single dose injection of ZnPc@Gel was evaluated in mice. As shown in Fig. 4a, in the control group, mice had a significant continuous increase in tumor volume over 15 days. The tumor volume at 15 days was about 14 times larger than the volume at baseline. In study groups, the tumor volume increased, with a lower rate compared with that in the control group. However, compared with the G3 group, the tumor volume in the other study groups treated with irradiation (G1UI group, G3UI group, G10UI group, M3UI group) was significantly reduced, which indicated higher cytotoxicity of ZnPc@Gel. The volume of tumors in the G3UI group increased with a lower rate than that in G1UI group and G10UI group. This result was due to the aggregation and photo-quenching of a high concentration of ZnPc. There was not significant difference in tumor growth curve between the G3UI group and M3UI group over 11 days. However, in the M3UI group, tumors grew faster after day 11. This result probably due to that the thermosensitive *in situ* gel as the carrier of ZnPc micelles effectively reduced tumor growth by improving drug retention in the tumors. The inhibition of tumor volume in DOX group was greater compared with that in other groups over study

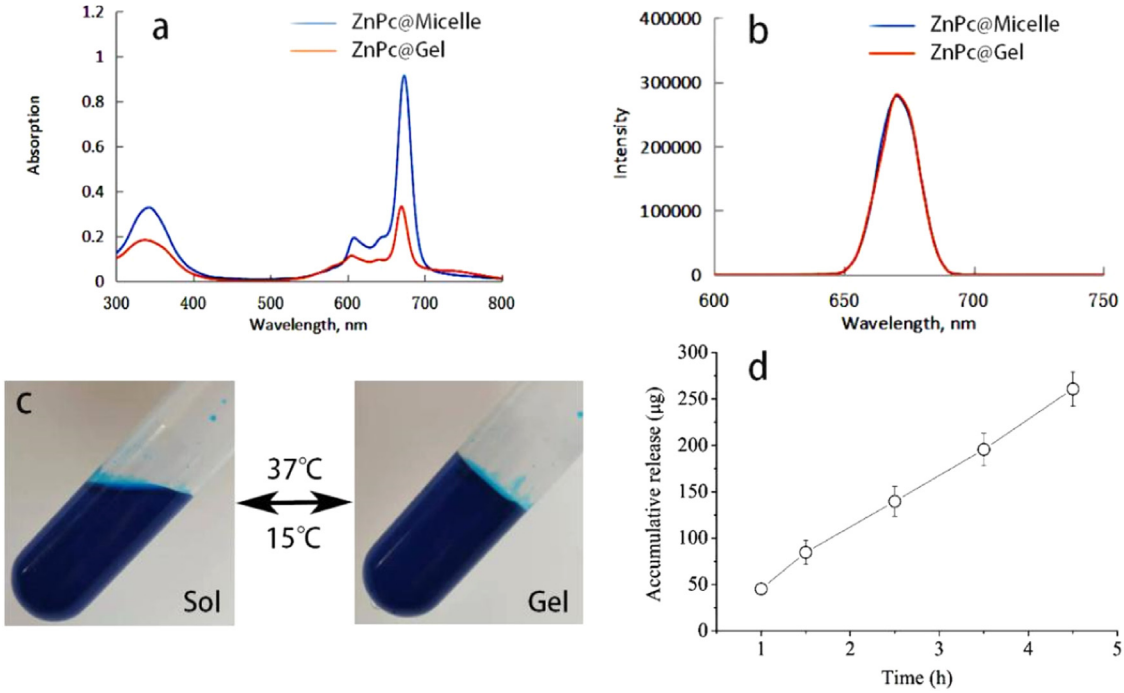

Fig. 2. Characterization of ZnPc@Micelle and ZnPc@Gel. (a) UV–vis spectrum of ZnPc@Micelle and ZnPc@Gel, (b) Fluorescence mission spectrum (excited at 670 nm) of ZnPc@Micelle and ZnPc@Gel, (c) Temperature-responsive sol-gel transition and (d) *in vitro* release profile of ZnPc@Gel.

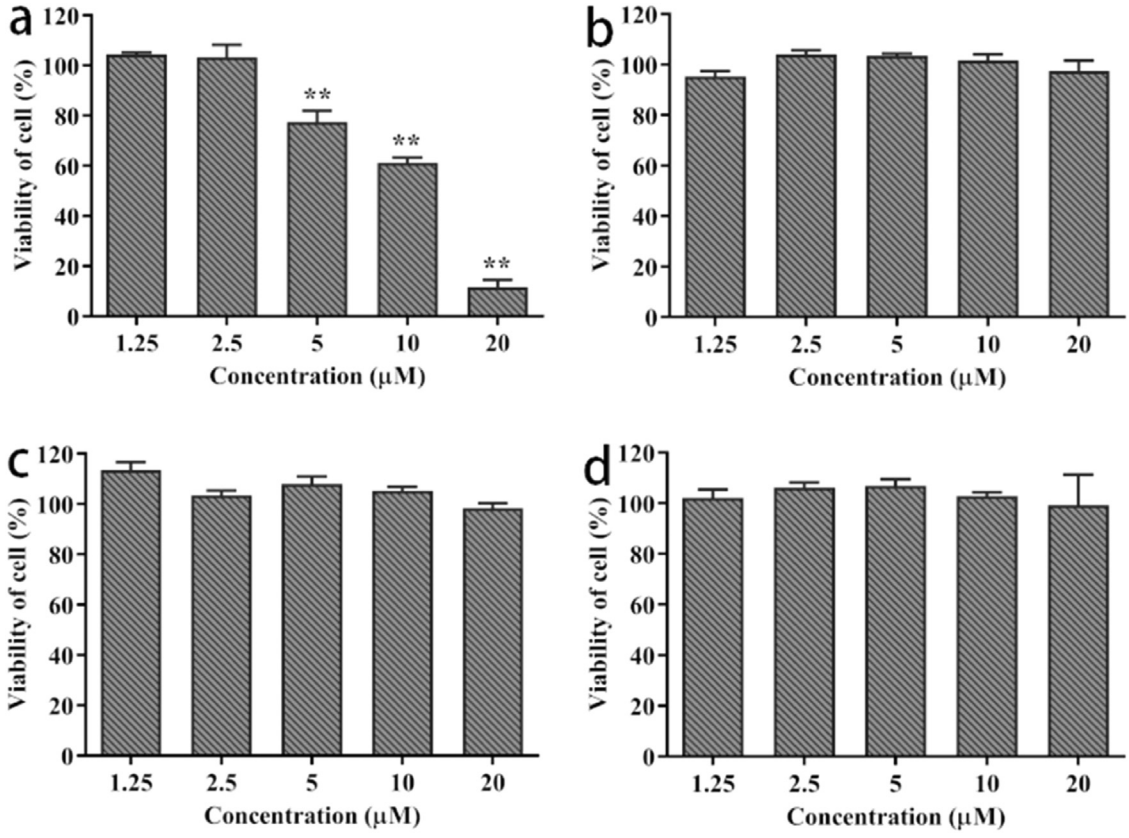

Fig. 3. Photodynamic antitumor toxicity effects of ZnPc@Gel and blank gel with/without irradiation on B16 cell line. (a) Cytotoxicity of ZnPc@Gel, (b) Dark toxicity of ZnPc@Gel, (c) Cytotoxicity of blank gel, (d) Dark toxicity of blank gel. The values shown represent mean ± SEM of three different assays ($n = 3$). * $P < 0.05$, ** $P < 0.01$ *vs.* control group.

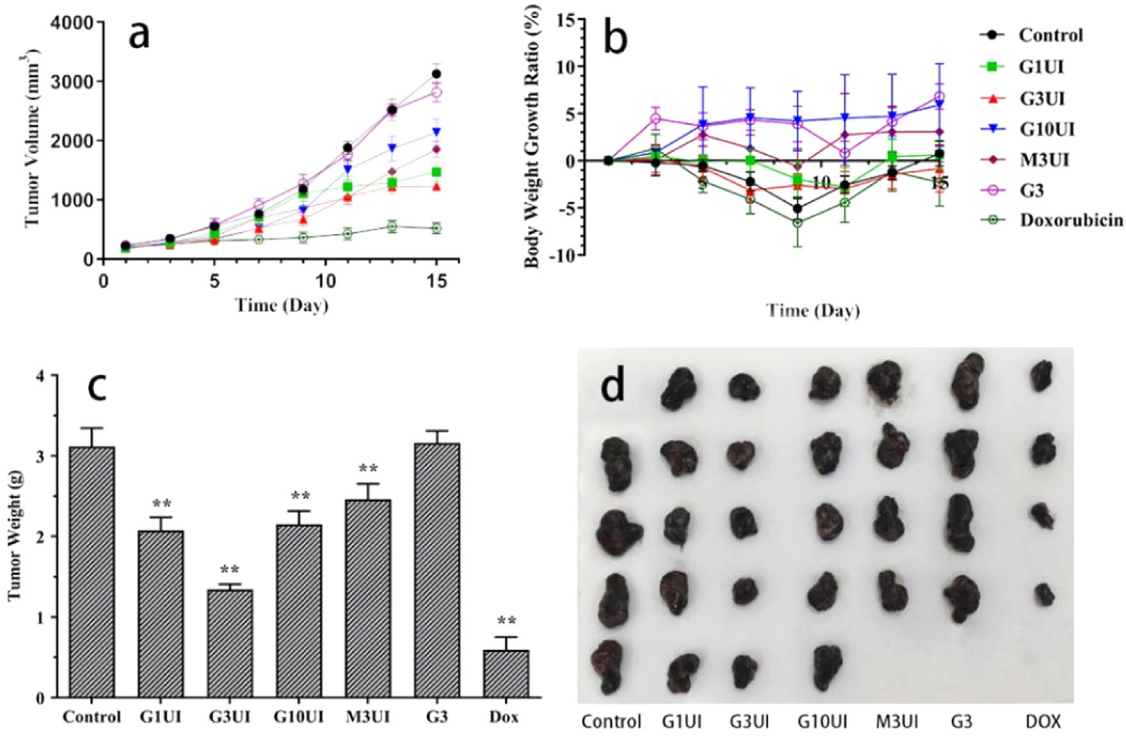

Fig. 4. The tumor volume (a), body weight (b), tumor weight (c), and tumor tissue morphology (d) of C57BL/6 mice bearing B16 after intratumoral injection of ZnPc *in situ* gel with/without irradiation. The values shown represent mean ± SEM (n = 4 or 5). * $P < 0.05$, ** $P < 0.01$ *vs*. control group, $^{\#\#}$ $P < 0.01$ *vs*. G3UI group.

period, with severe toxicity and the side effects, including one mouse dead at day 7.

As shown in Fig. 4b, the body weights of mice in the study and control groups were similar over study period. The mice in the control, G1UI, G3UI and doxorubicin groups had similar growth ratios of body weight. Body weights in these groups reduced from 0 to 9 days due to disease progression and increased from 10 to 15 days due to tumor growth. This trend was in line with the time pattern of tumor growth (Fig. 4a and b).

The anti-tumor efficacy of the ZnPc@Gel in PDT was evaluated using tumor weight, as shown in Fig. 4c, compared with the other groups, the G3UI and DOX groups had lower tumor weights with a tumor inhibition rate of 56.95 % and 80.94 %, respectively. As shown in Fig. 4d, both the G3UI and DOX groups had lower average tumor volume compared with other groups. The G3UI group had smaller average tumor size compared with that in the DOX group, which showed a nonuniform morphology.

The morphological changes of the tumors at 15 days were shown in Fig. 5. Tumors in the control group had a normal cell morphology. Minor necrosis was observed in tumors in the G3 group. The histological images in the G1UI and M3UI groups were similar, showing looser connections between cells compared with the control group. Widespread necrotic regions were observed in tumors in the G3UI and G10UI groups. The cell contraction was tighter in the G3UI group compared with the G10UI group. Consistent with the results in Fig. 4, the tumor damage in the DOX group was severe as tumor cells rarely connected with each other. The results demonstrated the efficacy of ZnPc@Gel PDT in melanoma.

Discussion

Melanoma is one of the most aggressive malignant tumors with unpredictable evolution, which is responsible for almost 79 % of skin cancer mortality.[25] Two main challenges of traditional PDT have limited the clinical application for the treatment of malignant melanoma[26,27]: light absorption of melanin and anti-oxidation of melanoma. Melanin acts as a physical filter for the most of PDT irradiation, which absorbs the light wavelength ranging 500~600 nm and

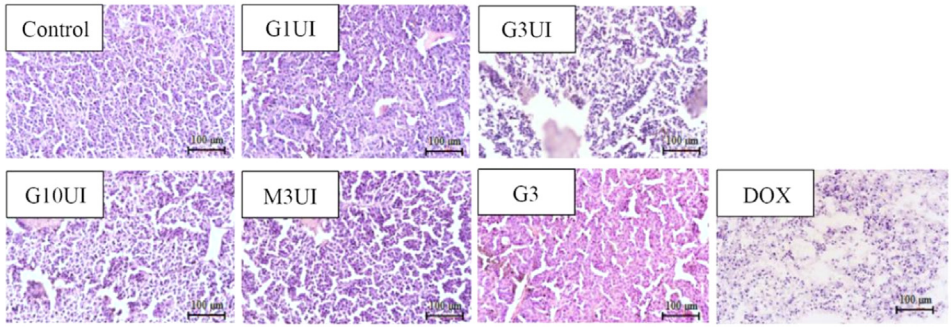

Fig. 5. The tumor cell morphology of C57BL/6 mice bearing B16 tumor after intratumoral injection of ZnPc@Gel with/without irradiation. Scale bar: 100 μm.

thus prevents in depth light penetration and activation of photosensitizers by therapeutic light in melanoma.[28] Therefore, photosensitizers cannot be activated due to a lack of adequate light. The antioxidant effect in melanoma is higher than that in other types of tumor and thus reduces the anti-tumor effect from ROS that generated by PDT. In this study, ZnPc was selected as the photosensitizer for PDT treatment of melanoma. ZnPc has a long peak activation wavelength (maximum absorption at about 670 nm), that avoids the absorbance of melanin and allows deeper tissue penetration. The intratumoral injection of ZnPc micelle-based thermo-sensitive *in situ* gel is a localized drug delivery system, improving the concentration of ZnPc in melanoma tumor and counteracting antioxidant effect of melanoma.

Although ZnPc is insoluble in water, the dispersibility of ZnPc was greatly improved in aqueous solution, containing TPGS. UV–Vis spectra showed that the maximum absorption peak of ZnPc in the aqueous solution containing 2 % TPGS was 670 nm similar to that in DMF and NMP, which indicated that ZnPc molecules were dispersed in this aqueous media. Another finding was that the addition of 2 % SDC in NMP increased the solubility of ZnPc. We prepared mixed micelles using SDC/TPGS as the drug carrier of ZnPc using solvent diffusion method (as shown in the Schematic diagram). In the hydrophobic core of micelles, the deoxycholate (DC) moiety of SDC and the hydrophobic segment of TPGS bounded with ZnPc and separated ZnPc molecules. This structure prevented the formation of π-π interaction between ZnPc molecules and improved the dispersion of ZnPc in aqueous solution. The ZnPc@Gel was prepared by adding F127 to the aqueous solution, which showed good dispersity through UV–Vis and fluorescence spectra. The assembly method and solvent influenced the stability of micelles. Lu et al. reported the preparation of ZnPc@Micelles using DMF as organic solvent and dialysis operation. This ZnPc@Micelles showed less obvious absorption at 670 nm and fluorescence characteristics of the micelles.[5] Compared with DMF, NMP used in this study improved the dispersibility of ZnPc. NMP is a pharmaceutical solvent approved by FDA and is not required to be removed from gels.

The results of *in vitro* cytotoxicity of ZnPc@Gel on B16 cells showed that PDT reduced cell viability. F127 and other micelle materials <20 μM had no toxicity and gel materials >20 μM inhibited the cell growth. The concentration of ZnPc@Gel of 40 μM significantly reduced the survival rate of the cells, regardless of in light or dark conditions. To evaluate the toxicity of high concentration gels, we performed the cell viability evaluation of the SDC-TPGS blank gel. The results demonstrated that the cytotoxicity on tumor cells was caused by the high weight and density of the high concentration gel. As shown in Fig. 3a and Fig. 6, the survival rate of tumor cells with ZnPc@Gel 40 μM was lower than that with ZnPc@Gel 20 μM. This result was attributed to the toxicity caused by the gel materials in ZnPc@Gel 40 μM rather than increased PDT effect *versus* ZnPc@Gel 20 μM. Indeed, the antitumor effects of PDT with 40 μM ZnPc@Gel decreased *versus* that with ZnPc@Gel 20 μM, which might be attributed to the aggregation of ZnPc. Therefore, the gel concentration is an important factor for PDT with ZnPc@Gel.

The G3UI and doxorubicin groups showed reductions in tumor weight and volume. Although the doxorubicin group had a higher tumor inhibition rate, toxicity on mice was higher compared with the G3UI group. Mice in the doxorubicin group gained less body weight during the experiment compared with the G3UI group, with one mouse dead at day 7. Unlike *in vitro* cytotoxicity results, pharmacodynamics results of ZnPc@Gel in tumor-xenografted mice showed no dose-dependent trend. The tumor weight and volume in the G10UI group were greater than those in the G3UI group due to the aggregation of high-concentration ZnPc in the tumor.

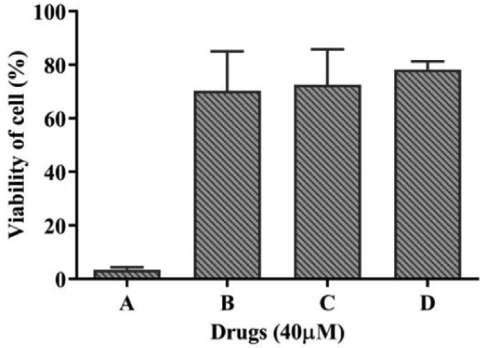

Fig. 6. Toxicity effects of high concentration (40 μM) ZnPc@Gel and blank gel with/without irradiation on B16 cell line. (A) Cytotoxicity of ZnPc@Gel; (B) Dark toxicity of ZnPc@Gel; (C) Cytotoxicity of blank gel; (D) Dark toxicity of blank gel. The values shown represent mean ± SEM of three different assays (n = 3).

PDT mediated cell death involves necrosis, apoptosis and/or autophagy pathways. To determine the mechanism of PDT-induced B16 cells death, different concentrations of ZnPc@Gel mixed with cells after PDT, stained using Hoechst 33342 nucleic acid stain were assessed. Fragmented nuclei with light blue were observed using inverted microscope and fluorescence microscope indicating apoptotic cells (Figure S1a and S1b). All ZnPc@Gel groups showed concentration-depended apoptosis. The control and ZnPc@Gel low dosage group (5 μM) showed few apoptotic cells whereas apoptotic cells significantly increased in high dosage groups (10 μM and 20 μM). The non-illumination 10 μM group showed few apoptotic cells compared with the 10 μM illumination group. This result was consistent with the PDT toxicity assay as shown in Fig. 3a. To confirm the apoptosis induced by ZnPc@Gel, after V-FITC/PI double staining, the cells were analyzed using a flow cytometer. As shown in Figure S1c, there were few necrotic cells. The early and late apoptosis in the ZnPc@Gel 10 μM and 20 μM illuminated groups were observed. ZnPc@Gel 10 μM and 20 μM illuminated groups showed a significantly higher rate than that in the non-illumination groups. This result demonstrated that ZnPc@Gel 10 μM and 20 μM induced a high level of apoptosis (Figure S1d). Many studies have reported that the reactive oxygen species (ROS) plays a key role in PDT and induced the cancer cells necrosis and/or apoptosis. ROS-mediated cellular oxidative stress, tissue anoxia and tumor starvation stop tumor vasculature and lead to an antitumor immune response. To analyze the relationship of ROS yield and apoptotic rate of tumor cells, we detected the ROS level using DCFH-DA probe. As shown in Figure S1e, the yield of ROS induced by 20 μM ZnPc@Gel solution was greatest among all the groups and was nearly two times of that in the 10 μM group. This concentration-dependent trend was consistent with the results assessed using V-FITC/PI double staining method (Figure S1f).

To verify the effects of ROS on cell survival rate and apoptosis, N-acetyl-L-cysteine (NAC), a ROS inhibitor, was used in this study. The cytotoxicity effects and apoptosis analysis of ZnPc@Gel were investigated using NAC as the ROS inhibitor. As shown in Figure S2 and Figure S3, the yield of ROS in all groups decreased to a low level after adding NAC, improving the survival rate and decreasing the amount of apoptosis on post-PDT tumor cells. The immunodetection of proteins, such as the expression of Caspase 3, Cleaved-caspase 3, Bax and Bcl-2 in the tumor tissues after PDT with ZnPc@Gel was detected using western blotting (Figure S4). Compared to the internal reference, the expression levels of Caspase3, cleaved-caspase3 and Bax increased significantly whereas that of Bcl-2 decreased in all irradiation groups. This result indicates that the apoptosis was the main mechanism for ZnPc@Gel PDT in melanoma.

Conclusions

In summary, to improve the water-solubility and antineoplastic effect of ZnPc in PDT, a ZnPc-loaded SDC-TPGS micelle, mixed with thermo-sensitive *in situ* gel was prepared. NMP is a good organic solvent for dissolving ZnPc to form micelles and gel. ZnPc@SDC-TPGS *in situ* gel had no toxicity in dark condition at a dose less than 40 μM and showed a dose-dependent phototoxicity. For ZnPc-mediated PDT, the yield of ROS and their derivatives subsequently oxidize biomolecules and play a key role in cellular demise and apoptosis. In the pharmacodynamic study in B16-bearing mice, intratumoral injection in the G3UI group led to better treatment efficiency compared with that in other groups. In conclusion, intratumoral administration of ZnPc@SDC-TPGS *in situ* gel for PDT demonstrated a good efficacy for the treatment of melanoma. ZnPc@SDC-TPGS *in situ* gel for intratumoral injection provides an alternative to melanoma therapy.

Declaration of Competing Interest

The authors declare that they have no known competing financial interests or personal relationships that could have appeared to influence the work reported in this paper.

Acknowledgements

This work was supported by the Key Scientific Research Project of Liaoning Province (grant no. 2021JH2/10300037), the Key Scientific Research Project of the Education Department of Liaoning (grant no.2019LZD01) and Scientific Research Project of Shenyang Medical College (grant no. 20171003). The authors thank Dr. Ye Tian for editing the manuscript as a medical writer and Mr. Zhao K.C. at Shanghai Chinaway Pharmaceutical Technology for kindly providing TPGS.

Supplementary materials

Supplementary material associated with this article can be found, in the online version, at doi:10.1016/j.xphs.2023.10.020.

References

1. Pucelik B, Arnaut LG, Stochel G, Dabrowski JM. Design of pluronic-based formulation for enhanced redaporfin-photodynamic therapy against pigmented melanoma. *ACS Appl Mater Interfaces*. 2016;8(34):22039–22055.
2. Wang X, Gong Q, Song C, et al. Berberine-photodynamic therapy sensitizes melanoma cells to cisplatin-induced apoptosis through ROS-mediated P38 MAPK pathways. *Toxicol Appl Pharmacol*. 2021;418: 115484.
3. Nakao S, Arai Y, Tasaki M, et al. Intratumoral expression of IL-7 and IL-12 using an oncolytic virus increases systemic sensitivity to immune checkpoint blockade. *Sci Transl Med*. 2020;12(526).
4. Li L, Luo Z, Chen Z, et al. Enhanced photodynamic efficacy of zinc phthalocyanine by conjugating to heptalysine. *Bioconjug Chem*. 2012;23(11):2168–2172.
5. Lu X, Zhu W, Chen T, Peng Q, Yu C, Yang M. Exploration of photophysical and photochemical properties of zinc phthalocyanine-loaded SDC/TPGS mixed micelles. *Chem Phys Lett*. 2019:735.
6. Chen Z, Zhou S, Chen J, et al. An effective zinc phthalocyanine derivative for photodynamic antimicrobial chemotherapy. *J Lumin*. 2014;152:103–107.
7. Yu W, Ye M, Zhu J, et al. Zinc phthalocyanine encapsulated in polymer micelles as a potent photosensitizer for the photodynamic therapy of osteosarcoma. *Nanomedicine*. 2018;14(4):1099–1110.
8. Wang Z, Gai S, Wang C, et al. Self-assembled zinc phthalocyanine nanoparticles as excellent photothermal/photodynamic synergistic agent for antitumor treatment. *Chem Eng J*. 2019;361:117–128.
9. Saw CL, Heng PW, Chin WW, Soo KC, Olivo M. Enhanced photodynamic activity of hypericin by penetration enhancer N-methyl pyrrolidone formulations in the chick chorioallantoic membrane model. *Cancer Lett*. 2006;238(1):104–110.
10. Gu X, Shen C, Li H, Goldys EM, Deng W. X-ray induced photodynamic therapy (PDT) with a mitochondria-targeted liposome delivery system. *J Nanobiotechnology*. 2020;18(1):87.
11. Liu X, Yang Y, Wang X, et al. Self-assembled Au4Cu4/Au25 NCs@liposome tumor nanotheranostics with PT/fluorescence imaging-guided synergetic PTT/PDT. *J Mater Chem B*. 2021;9(32):6396–6405.
12. Choudhury H, Gorain B, Pandey M, et al. Recent advances in TPGS-based nanoparticles of docetaxel for improved chemotherapy. *Int J Pharm*. 2017;529(1–2): 506–522.
13. Sun S, Du X, Fu M, et al. Galactosamine-modified PEG-PLA/TPGS micelles for the oral delivery of curcumin. *Int J Pharm*. 2021;595: 120227.
14. Huang C, Chen F, Zhang L, Yang Y, Yang X, Pan W. ^{99m}Tc radiolabeled HA/TPGS-based curcumin-loaded nanoparticle for breast cancer synergistic theranostics: design, *in vitro* and *in vivo* evaluation. *Int J Nanomedicine*. 2020;15:2987–2998.
15. Singla P, Singh O, Chabba S, Aswal VK, Mahajan RK. Sodium deoxycholate mediated enhanced solubilization and stability of hydrophobic drug Clozapine in pluronic micelles. *Spectrochim Acta A Mol Biomol Spectrosc*. 2018;191:143–154.
16. Haque ME, Das AR, Moulik SP. Mixed micelles of sodium deoxycholate and polyoxyethylene sorbitan monooleate (Tween 80). *J Colloid Interface Sci*. 1999;217 (1):1–7.
17. Patel V, Ray D, Bahadur A, Ma J, Aswal VK, Bahadur P. Pluronic((R))-bile salt mixed micelles. *Colloids Surf B Biointerfaces*. 2018;166:119–126.
18. Cross D, Burmester JK. Gene therapy for cancer treatment: past, present and future. *Clin Med Res*. 2006;4(3):218–227.
19. Vegt PD, Debruyne FM, Van Der Meijden AP. Bacillus Calmette-Guerin in superficial bladder cancer: consensus and controversies. *Eur Urol*. 1995;27(2):89–95.
20. Guo J, Wang J, Cai C, et al. The anti-melanoma efficiency of the intratumoral injection of cucurbitacin-loaded sustained release carriers: in situ-forming implants. *AAPS PharmSciTech*. 2015;16(4):973–985.
21. Wang JW, Xu JH, Li J, Zhao MH, Zhang HF, Liu DC, et al. Improvement of the antitumor efficacy of intratumoral administration of cucurbitacin poly (lactic-co-glycolic acid) microspheres incorporated in in situ-forming sucrose acetate isobutyrate depots. *J Pharm Sci*. 2016;105(1):205–211.
22. Westphal M, Hilt DC, Bortey E, et al. A phase 3 trial of local chemotherapy with biodegradable carmustine (BCNU) wafers (Gliadel wafers) in patients with primary malignant glioma. *Neuro Oncol*. 2003;5(2):79–88.
23. Yu M, Zhang C, Tang Z, Tang X, Xu H. Intratumoral injection of gels containing losartan microspheres and (PLG-g-mPEG)-cisplatin nanoparticles improves drug penetration, retention and anti-tumor activity. *Cancer Lett*. 2019;442:396–408.
24. Castro DJ, Sridhar KS, Garewal HS, et al. Intratumoral cisplatin/epinephrine gel in advanced head and neck cancer: a multicenter, randomized, double-blind, phase III study in North America. *Head Neck*. 2003;25(9):717–731.
25. Slominski AT, Carlson JA. Melanoma resistance: a bright future for academicians and a challenge for patient advocates. *Mayo Clin Proc*. 2014;89(4):429–433.
26. Huang YY, Vecchio D, Avci P, Yin R, Garcia-Diaz M, Hamblin MR. Melanoma resistance to photodynamic therapy: new insights. *Biol Chem*. 2013;394(2):239–250.
27. Monge-Fuentes V, Muehlmann LA, De Azevedo R B. Perspectives on the application of nanotechnology in photodynamic therapy for the treatment of melanoma. *Nano Rev*. 2014;5.
28. Hadjur C, Richard MJ, Parat MO, Jardon P, Favier A. Photodynamic effects of hypericin on lipid peroxidation and antioxidant status in melanoma cells. *Photochem Photobiol*. 1996;64(2):375–381.